SUPPLEMENTARY INFORMATION

These set of notes describe cavity optomechanics in the presence of additional thermo-optic tuning of the cavity resonance. We find that thermo-optic tuning results in correction factors to both the optical spring and optomechanical gain. In addition there is an overall saturation of the optomechanical coupling. These effects can be large for systems with large static thermo-optic tuning and fast thermal decay relative to the mechanical frequency (i.e., small heat capacity). Analysis of the zipper optomechanical cavity indicates that optical damping can be realized with blue detuned light, in direct opposition to the bare optomechanical effect. Several, supporting measurements/calculations are also presented, including estimates of the quantum back-action noise and thermo-mechanical effects, both found to be negligible on the scale of the measured properties of the zipper cavity system, and measurement of the zipper cavity mechanical Q-factor in vacuum ($Q_{M,\mathrm{vac}} > 10^4$). Finally, methods and parameters used in fitting a steady-state nonlinear optical model, including the gradient optical force and thermo-optic tuning, to the measured zipper optomechanical cavity response are provided at the end of the notes.

PACS numbers:

I. THERMO-OPTIC EFFECTS

A. Coupled mode theory

We begin with the set of coupled equations describing mechanical and optical motion,

$$\dot{a} = -(i(\Delta_o - g_{\mathrm{OM}}x) + \Gamma/2)a + \kappa s, \tag{S-1}$$

$$\ddot{x} = -\gamma_M \dot{x} - \Omega_M^2 x - \frac{|a|^2 g_{\mathrm{OM}}}{\omega_o m_x}, \tag{S-2}$$

where $\Delta_o \equiv (\omega_l - \omega_o)$ is the bare laser detuning from the optical cavity resonance (ω_o), Γ is the optical cavity (energy) decay rate, $\kappa(=\sqrt{1/\tau_e})$ is the input coupling rate of the laser into the cavity, $|s|^2$ is the optical input power, $g_{\mathrm{OM}} \equiv \mathrm{d}\omega/\mathrm{d}x$ is the optomechanical factor, γ_M is the bare mechanical (energy) damping factor, $\Omega_M(=\sqrt{k/m_x})$ is the bare mechanical frequency, m_x is the bare motional mass of the mechanical resonator, and a is the amplitude of the optical cavity field normalized so that $|a|^2$ represents the stored optical cavity energy. The equation for a is written in a slowly varying basis in which the laser frequency, ω_l, has been removed from both a and s.

In order to include the effects of thermo-optic tuning of the cavity resonance, we include a third equation for the cavity temperature increase, ΔT:

$$\dot{a} = -(i(\Delta_o - (g_{\mathrm{OM}}x + g_{th}\Delta T)) + \Gamma/2)a + \kappa s, \tag{S-3}$$

$$\ddot{x} = -\gamma_M \dot{x} - \Omega_M^2 x - \frac{|a|^2 g_{\mathrm{OM}}}{\omega_o m_x}, \tag{S-4}$$

$$\dot{\Delta T} = -\gamma_{th}\Delta T + \Gamma_{abs}|a|^2 c_{th}, \tag{S-5}$$

where $g_{th} = -(\mathrm{d}n/\mathrm{d}T)(\omega_o/n_o)$ is the thermo-optic tuning coefficient, $\mathrm{d}n/\mathrm{d}T$ is the thermo-optic coefficient of the optical and mechanical cavity material, Γ_{abs} is the component of the optical energy decay which is due to material absorption, c_{th} is the thermal heat capacity of the cavity, and γ_{th} is temperature decay rate.

In order to solve these coupled equations we proceed using a perturbation approach[1]. We assume that the mechanical motion is harmonic in time with small amplitude parameter ε_x, $x(t) = x_o + \varepsilon_x \cos(\Omega_M t)$. The optical cavity mode amplitude and the cavity temperature increase can be expanded in terms of the small parameter ε_x,

$$a(x,t) = \sum_{n=0}^{\infty} \varepsilon_x^n a_n(x,t), \tag{S-6}$$

$$\Delta T(x,t) = \sum_{n=0}^{\infty} \varepsilon_x^n \Delta T_n(x,t). \tag{S-7}$$

$$\tag{S-8}$$

Keeping terms only to first order in ε_x yields the following sets of coupled equations,

$$0 = -(i\Delta_o' + \Gamma/2)a_0 + \kappa s, \tag{S-9}$$

$$0 = -\Omega_M^2 x_o - \frac{|a_0|^2 g_{\mathrm{OM}}}{\omega_o m_x}, \tag{S-10}$$

$$0 = -\gamma_{th}\Delta T_o + \Gamma_{abs}|a_0|^2 c_{th}, \tag{S-11}$$

and

$$\dot{a}_1 = +i(g_{\mathrm{OM}}x_1 + g_{th}\Delta T_1))a_0 - (i\Delta_o' + \Gamma/2)a_1, \tag{S-12}$$

$$\ddot{x_1} = -\gamma_M \dot{x}_1 - \Omega_M^2 x_1 - \frac{(a_0 a_1^* + a_0^* a_1)g_{\mathrm{OM}}}{\omega_o m_x}, \tag{S-13}$$

$$\dot{\Delta T}_1 = -\gamma_{th}\Delta T_1 + \Gamma_{abs}(a_0 a_1^* + a_0^* a_1)c_{th}, \tag{S-14}$$

where $x_1 \equiv \cos(\Omega_M t)$ and $\Delta_o' = \Delta_o - (g_{\mathrm{OM}}x_o + g_{th}\Delta T_o)$ is the time averaged laser-cavity detuning. Fourier transforming the first-order perturbation equations to convert them from differential to algebraic ones yields,

$$(i(\omega + \Delta_o') + \Gamma/2)\tilde{a}_1 = +i(g_{\mathrm{OM}}\tilde{x}_1 + g_{th}\tilde{\Delta T}_1)a_0, \tag{S-15}$$

$$(i(\omega - \Delta_o') + \Gamma/2)\tilde{a_1^*} = -i(g_{\mathrm{OM}}\tilde{x}_1 + g_{th}\tilde{\Delta T}_1)a_0^*, \tag{S-16}$$

$$-\omega^2\tilde{x}_1 = -i\omega\gamma_M\tilde{x}_1 - \Omega_M^2\tilde{x}_1 - \frac{(a_0\tilde{a_1^*} + a_0^*\tilde{a}_1)g_{\mathrm{OM}}}{\omega_o m_x}, \tag{S-17}$$

$$(i\omega + \gamma_{th})\tilde{\Delta T}_1 = \Gamma_{abs}(a_0\tilde{a_1^*} + a_0^*\tilde{a}_1)c_{th}, \tag{S-18}$$

Solving for the time-dependent part of the optical cavity energy,

$$(a_0\tilde{a_1^*} + a_0^*\tilde{a}_1) = f(\omega, \Delta_o')\left[i|a_0|^2(g_{\mathrm{OM}}\tilde{x}_1 + g_{th}\tilde{\Delta T}_1)\right], \tag{S-19}$$

where we have defined the transfer function f as,

$$f(\omega, \Delta_o') = \left(\frac{1}{(i(\omega + \Delta_o') + \Gamma/2)} - \frac{1}{(i(\omega - \Delta_o') + \Gamma/2)}\right). \tag{S-20}$$

Substituting for $\tilde{\Delta T}_1$ of eq. (S-18) allows us to solve for the optical cavity energy solely in terms of the mechanical motion,

$$\left(f(\omega, \Delta_o')^{-1} - i\frac{g_{th}\Gamma_{abs}c_{th}|a_0|^2}{i\omega + \gamma_{th}}\right)(a_0\tilde{a_1^*} + a_0^*\tilde{a}_1) = i|a_0|^2 g_{\mathrm{OM}}\tilde{x}_1. \tag{S-21}$$

Defining $f'(\omega, |a_0|^2)$ and $g(\omega, \Delta_o', |a_0|^2)$ as,

$$f'(\omega, |a_0|^2) = -i\frac{g_{th}\Gamma_{abs}c_{th}|a_0|^2}{i\omega + \gamma_{th}}, \tag{S-22}$$

$$g(\omega, \Delta_o', |a_0|^2) = f\left[\frac{1 + (f')^* f^*}{|1 + f' f|^2}\right], \tag{S-23}$$

allows us to write for the Fourier transform of the time varying component of the cavity energy,

$$(a_0\tilde{a_1^*}+a_0^*\tilde{a}_1) = ig(\omega,\Delta_o',|a_0|^2)|a_0|^2 g_{\rm OM}\tilde{x}_1. \tag{S-24}$$

All of the transfer functions f, f', and g have the property that $h(-\omega) = -h(\omega)^*$. With $\tilde{x}_1 = (\delta(\omega-\Omega_M)+\delta(\omega-\Omega_M)/2$, we have for the cavity energy,

$$(a_0\tilde{a_1^*}+a_0^*\tilde{a}_1) = i|a_0|^2 g_{\rm OM}(g(\Omega_M)\delta(\omega-\Omega_M)+g(-\Omega_M)\delta(\omega+\Omega_M))/2 \tag{S-25}$$

$$= -\frac{|a_0|^2 g_{\rm OM}(g(\Omega_M)\delta(\omega-\Omega_M)-g^*(\Omega_M)\delta(\omega+\Omega_M))}{2i}. \tag{S-26}$$

Further symplifying this result yields,

$$(a_0\tilde{a_1^*}+a_0^*\tilde{a}_1) = -|a_0|^2 g_{\rm OM}\left[\frac{{\rm Re}(g(\Omega_M))(\delta(\omega-\Omega_M)-\delta(\omega+\Omega_M))}{2i}+\frac{{\rm Im}(g(\Omega_M))(\delta(\omega-\Omega_M)+\delta(\omega+\Omega_M))}{2}\right]. \tag{S-27}$$

Finally this gives in the time-domain,

$$(a_0 a_1^*(t)+a_0^* a_1(t)) = |a_0|^2 g_{\rm OM}\left[\frac{{\rm Re}(g(\Omega_M))}{\Omega_M}(-\Omega_M\sin\Omega_M t)-{\rm Im}(g(\Omega_M))\cos\Omega_M t\right], \tag{S-28}$$

$$= |a_0|^2 g_{\rm OM}\left[\frac{{\rm Re}(g(\Omega_M))}{\Omega_M}\dot{x}_1-{\rm Im}(g(\Omega_M))x_1\right] \tag{S-29}$$

Substituting this result into the equation of motion for $x_1(t)$ in eq. (S-13) allows one to identify renormalized mechanical frequency (Ω_M') and damping (γ_M') terms due to optomechanical and thermo-optic interactions,

$$(\Omega_M')^2 = \Omega_M^2-\frac{|a_0|^2 g_{\rm OM}^2{\rm Im}(g(\Omega_M))}{\omega_o m_x}, \tag{S-30}$$

$$\gamma_M' = \gamma_M+\frac{|a_0|^2 g_{\rm OM}^2{\rm Re}(g(\Omega_M))}{\Omega_M\omega_o m_x}. \tag{S-31}$$

The effects of the thermo-optic tuning of the cavity are manifest in the correction to the pure optomechanical transfer function (f) in the equation for g given in eq. (S-23). This correction factor is simply $1/(1+f'f)$. For $|f'f|\ll 1$ the thermo-optic correction is small, and can be neglected. In order to make connection with previously derived results for the optomechanical spring and gain coefficient, we now consider this correction in the sideband unresolved limit, relevant for the current zipper cavities.

B. Sideband unresolved limit ($\Omega_M \ll \Gamma$)

We begin by evaluating $f(\Omega_M)$ in the limit that $\Omega_M \ll \Gamma$,

$$f(\Omega_M) \approx -2\Delta_o'\left(\frac{\Gamma\Omega_M+i\Delta^2}{\Delta^4}\right), \tag{S-32}$$

where we have defined $\Delta^2 = (\Delta_o')^2+(\Gamma/2)^2$. In the absence of thermo-optic tuning this results in the usual equations for the sideband unresolved optical spring effect and optomechanical gain,

$$(\Omega_M')^2|_{\Delta T_1=0} = \Omega_M^2+\left(\frac{2|a_0|^2 g_{\rm OM}^2}{\Delta^2\omega_o m_x}\right)\Delta_o', \tag{S-33}$$

$$\gamma_M'|_{\Delta T_1=0} = \gamma_M-\left(\frac{2|a_0|^2 g_{\rm OM}^2\Gamma}{\Delta^4\omega_o m_x}\right)\Delta_o'. \tag{S-34}$$

As can be seen, this results in an increase in the mechanical frequency and negative damping (positive *gain*) of the mechanical motion for blue detuned laser light (relative to the steady-state cavity resonance frequency).

We now consider the thermo-optic response in the case where the mechanical frequency is much larger than the thermal decay rate, a situation commonly found in optomechanical microsystems. We begin with f',

$$f'(\Omega_M) = (-\Omega_M\gamma_{th} - i\gamma_{th}^2)\left(\frac{\Delta_{th}}{\Omega_M^2+\gamma_{th}^2}\right) \approx (-\Omega_M\gamma_{th} - i\gamma_{th}^2)\left(\frac{\Delta_{th}}{\Omega_M^2}\right), \tag{S-35}$$

where we have assumed that the mechanical frequency is much larger than the thermal decay rate ($\Omega_M \gg \gamma_{th}$) and we have associated $g_{th}\Gamma_{abs}c_{th}|a_0|^2/\gamma_{th}$ with the static thermo-optic tuning of the cavity resonance, Δ_{th}. In order to evaluate g, we need the unresolved sideband limit of $|f|^2$, $|f'|^2$, and $2\mathrm{Re}(f'f)$,

$$|f(\Omega_M)|^2 \approx \frac{4(\Delta_o')^2}{\Delta^4}, \tag{S-36}$$

$$|f'(\Omega_M)|^2 \approx \left(\frac{\gamma_{th}\Delta_{th}}{\Omega_M}\right)^2, \tag{S-37}$$

$$2\mathrm{Re}(f'(\Omega_M)f(\Omega_M)) \approx \frac{4\Delta_o'\Delta_{th}\gamma_{th}(\Delta^2\gamma_{th} - \Omega_M^2\Gamma)}{\Omega_M^2\Delta^4}. \tag{S-38}$$

This yields for the transfer function $g(\Omega_M)$ in the sideband unresolved limit and for $\Omega_M \gg \gamma_{th}$,

$$g(\Omega_M) \approx \left(\frac{1}{1+s(|a_o|^2)}\right)\left(f(\Omega_M) + \frac{4(f'(\Omega_M))^*(\Delta_o')^2}{\Delta^4}\right), \tag{S-39}$$

where we have defined a saturation parameter, s, which is equal to,

$$s \approx \left(\frac{2\Delta_o'\gamma_{th}\Delta_{th}(|a_0|^2)}{\Delta^2\Omega_M}\right)^2\left(1 + \left(\Delta_{th}(|a_0|^2)\right)^{-1}\left(\frac{\Delta^2}{\Delta_o'} - \frac{\Omega_M^2\Gamma}{\Delta_o'\gamma_{th}}\right)\right). \tag{S-40}$$

Under most situations in which the thermo-optic correction to the bare optomechanics is significant, the static thermo-optic tuning of the cavity resonance dominates all other rates and only the first term contributes to s,

$$s \approx \left(\frac{2\Delta_o'\gamma_{th}\Delta_{th}(|a_0|^2)}{\Delta^2\Omega_M}\right)^2. \tag{S-41}$$

One can usefully relate the thermo-optic correction factor in eq. (S-39) to that of the bare optomechanical factor f as,

$$\frac{4(f'(\Omega_M))^*(\Delta_o')^2}{\Delta^4} \approx \mathrm{Re}(f(\Omega_M))\left(\frac{2\Delta_{th}\Delta_o'\gamma_{th}}{\Omega_M^2\Gamma}\right) + i\mathrm{Im}(f(\Omega_M))\left(\frac{-2\Delta_{th}\Delta_o'\gamma_{th}^2}{\Delta^2\Omega_M^2}\right). \tag{S-42}$$

Substituting eqs. (S-35,S-39) into eqs. (S-30,S-31) yields the following thermo-optic corrections to the optical spring and optomechanical gain coefficients in the sideband unresolved limit and for slow thermal response,

$$(\Omega_M')^2 \approx \Omega_M^2 + \left(\frac{2|a_0|^2 g_{\mathrm{OM}}^2\Delta_o'}{\Delta^2\omega_o m_x}\right)\left[\frac{1+W}{1+s}\right], \tag{S-43}$$

$$\gamma_M' \approx \gamma_M - \left(\frac{|a_0|^2 g_{\mathrm{OM}}^2\Gamma\Delta_o'}{\Delta^4\omega_o m_x}\right)\left[\frac{1+V}{1+s}\right], \tag{S-44}$$

where the correction factors are,

$$W = -\left(\frac{2\Delta_{th}\Delta_o'\gamma_{th}^2}{\Delta^2\Omega_M^2}\right) = -\left(\frac{2\Delta_{th}}{\Gamma}\right)\left(\frac{\gamma_{th}}{\Omega_M}\right)^2\left(\frac{\Gamma\Delta_o'}{\Delta^2}\right), \tag{S-45}$$

$$V = \left(\frac{2\Delta_{th}\Delta_o'\gamma_{th}}{\Omega_M^2\Gamma}\right) = \left(\frac{2\Delta_{th}}{\Gamma}\right)\left(\frac{\gamma_{th}}{\Omega_M}\right)^2\left(\frac{\Delta_o'}{\gamma_{th}}\right). \tag{S-46}$$

It should be noted that both W and V are dependent upon the (time) average stored cavity energy through the static thermo-optic tuning, Δ_{th}. It is also noteworthy that since the thermo-optic tuning is negative for most cavity materials (heat generates a red shift of the cavity resonance), W will be a positive quantity and V a negative one for blue detuned laser input ($\Delta'_o > 0$). In this way the thermo-optic correction tends to increase the bare optical spring effect and reduce the bare optomechanical gain when one tunes to the blue side of the cavity resonance. This negative correction to the optomechanical gain can then result in an effective mechanical damping on the stable blue-detuned side of the cavity resonance if $|V| > 1$, a case study of which will be explored below. The situation is reversed for a red detuned laser input, with the optical spring effect tending to be reduced and the optomechanical damping being enhanced.

Before proceeding to study specific examples, it is useful to estimate the correction factors and the saturation parameter for detunings close to the maximal bare optomechanical response, $|\Delta'_o| \approx \Gamma/2$. Substituting this detuning into eqs. (S-41,S-45,S-46) yields,

$$|s(|\Delta'_o| = \Gamma/2)| \approx \left(\frac{2\Delta_{th}}{\Gamma}\right)^2 \left(\frac{\gamma_{th}}{\Omega_M}\right)^2, \tag{S-47}$$

$$|W(|\Delta'_o| = \Gamma/2)| \approx \left(\frac{2|\Delta_{th}|}{\Gamma}\right) \left(\frac{\gamma_{th}}{\Omega_M}\right)^2, \tag{S-48}$$

$$|V(|\Delta'_o| = \Gamma/2)| \approx \left(\frac{2|\Delta_{th}|}{\Gamma}\right) \left(\frac{\gamma_{th}}{\Omega_M}\right)^2 \left(\frac{\Gamma}{2\gamma_{th}}\right). \tag{S-49}$$

The correction factor to the optomechanical gain (damping) is seen to be $\Gamma/2\gamma_{th}$ times larger than that of the correction to the optical spring effect. For optomechanical systems of micron scale and high optical Q, $\Gamma/2\pi \sim 10$ MHz and $\gamma_{th}/2\pi \sim 10$ kHz are reasonable numbers, which means the gain correction is on the order of a thousand times larger than the spring correction. For more modest optical Q systems ($Q \sim 10^5$), the gain correction is a million times larger than the spring correction. The saturation parameter scales similarly to the optical spring correction factor, with an extra factor of $2\Delta_{th}/\Gamma$. Thus, for static thermo-optic tuning greater than the cavity linewidth (thermo-optic bistability) the optical spring correction due to thermo-optic tuning *always* serves to quench the bare optomechanical effect. The optomechanical gain (damping), however, can be enhanced over a useful parameter regime. We now proceed to analyze the thermo-optic effects on the properties of the *zipper* optomechanical cavity.

C. The *zipper* optomechanical cavity

The zipper cavity studied in the manuscript has an optical Q-factor on the order of $Q \sim 3 \times 10^4$ ($\Gamma/2\pi \sim 6$ GHz or roughly a $\delta\lambda \sim 50$ pm linewidth), a mechanical frequency $\Omega_M/2\pi \sim 10$ MHz, and a thermal decay rate of roughly $\gamma_{th}/2\pi \sim 8$ kHz (see below). These devices have significant optical absorption at $\lambda \sim 1550$ nm, resulting in a static thermo-optic tuning of roughly $\Delta\lambda_{th} \sim 4$ nm (100 cavity linewidths) for a time-averaged stored cavity energy of 3 fJ ($P_i \sim 5$ mW). The correction and saturation parameters for the zipper cavity under this sort of optical input power and at the "optimal" detuning are,

$$|s(|\Delta'_o| = \Gamma/2)| \approx 2 \times 10^{-3}, \tag{S-50}$$

$$|W(|\Delta'_o| = \Gamma/2)| \approx 8 \times 10^{-6}, \tag{S-51}$$

$$|V(|\Delta'_o| = \Gamma/2)| \approx 10. \tag{S-52}$$

We see that, because of the large thermo-optic tuning and reasonably fast thermal response (a result of the small heat capacity), for the zipper cavity the optomechanical gain reverses sign at high enough optical input power for blue detuned pumping, resulting in strong optomechanical damping of the mechanical motion. This is what we see in our measurements. The optical spring is left unaffected and the overall saturation of the optomechanical coupling is negligible.

II. QUANTUM BACK-ACTION NOISE

Quantum back-action on the mechanical oscillator, due to the quantum fluctuations of the internal optical cavity field, results in an effective standard quantum limit (SQL) to which the mechanical oscillator's position can be determined[2]. Most analyses concerning quantum back-action noise in cavity-optomechanical systems are specific to the scattering radiation pressure force in which the optical cavity length is intimately related to the optomechanical coupling factor. This results in relations that depend upon cavity Finesse instead of cavity Q. Cavity-optomechanical systems that utilize gradient optical forces have an optomechanical coupling that scales with the inverse of a length, $L_{\rm OM}$, related to the transverse geometry of the cavity. As

such, all optomechanical relations end up more naturally being couched in terms of cavity Q and $L_{\rm OM}$ (or $g_{\rm OM}$). In the case of quantum back-action noise, for "measurement" times much longer than the mechanical decay time and in the bad cavity limit, the displacement noise power spectral density due to radiation force fluctuations within the cavity can be written as (following an analysis similar to Ref. [2]),

$$S_x^{\rm BA}\left(\Omega/2\pi;\Delta_o=\frac{\Gamma}{2\sqrt{3}}\right)=6\hbar g_{\rm OM}^2\frac{KQ^2}{\omega_o^3}\chi_M^2(\Omega)P_d, \tag{S-53}$$

where $Q\equiv\omega_o/\Gamma$ is the *loaded* optical cavity Q-factor, K (≈ 0.1 for our measurements) is a coupling parameter describing the strength of the cavity loading by the fiber taper waveguide[3], and the mechanical susceptibility is given by, $\chi_M^2(\Omega)=(m_x^2(\Omega^2-\Omega_M^2)^2+m_x^2\Omega^2\Omega_M^2/Q_M^2)^{-1}$. In deriving this relation we have assumed the laser-to-cavity detuning is chosen at the optimal point (in terms of transducing mechanical motion via detection of the transmitted laser power) of $\Delta_o=\Gamma/2\sqrt{3}$. At this detuning the dropped optical power into the cavity is $P_d=(3/4)(4K/(1+K)^2)P_i$, where P_i is the input optical power to the cavity. The thermal displacement noise power spectral density is given by the well known one-sided spectral density,

$$S_x^{\rm th}(\Omega/2\pi)=\frac{4k_BTm_x\Omega_M}{Q_M}\chi_M^2(\Omega). \tag{S-54}$$

The ratio $S_x^{\rm BA}(\Omega/2\pi)/S_x^{\rm th}(\Omega/2\pi)$ defines the relevance of the quantum back-action noise in the presence of thermally-induced Brownian motion, which for our measurement geometry (under optimal detuning) is given as,

$$\frac{S_x^{\rm BA}\left(\Omega/2\pi;\Delta_o=\frac{\Gamma}{2\sqrt{3}}\right)}{S_x^{\rm th}(\Omega/2\pi)}=\left(\frac{6\hbar g_{\rm OM}^2KQ^2Q_M}{4k_BTm_x\Omega_M\omega_o^3}\right)P_d. \tag{S-55}$$

Evaluating this ratio for the zipper cavity optomechanical system studied in this work, we find $S_{\rm BA}/S_{\rm therm}\approx 0.03$ per Watt of dropped optical cavity power at a bath temperature of $T=300$ K. The largest optical power used in the experiments described in this work is $P_i=5$ mW, roughly four orders of magnitude below that required to produce significant quantum back-action noise (on the scale of the thermal noise) for the zipper cavity at room temperature.

In addition to quantum back-action and thermal noise, the ultimate displacement sensitivity is also limited by the optical noise and electrical noise involved with the measurement of the optical signal. For the direct photodetection of the transmitted optical intensity of the zipper cavity used in this work, one can show that the *resonant* effective displacement noise power spectral densities for shot-noise-limited ($S_{\rm SN}$; not performed in our work) and photoreceiver-noise-limited detection ($S_{\rm PD}$; the NEP of our detector is 2.5 pW/Hz$^{1/2}$ at the frequency of the h_{1d} mode) are:

$$S_x^{\rm SN}\left(\Omega_M/2\pi;\Delta_o=\frac{\Gamma}{2\sqrt{3}}\right)=\left(\frac{2\hbar\omega_o^3\left(\frac{(1+K)^2}{3K}-1\right)}{3\eta g_{\rm OM}^2Q^2}\right)P_d^{-1}, \tag{S-56}$$

$$S_x^{\rm PD}\left(\Omega_M/2\pi;\Delta_o=\frac{\Gamma}{2\sqrt{3}}\right)=\left(\frac{2\omega_o^2}{3g_{\rm OM}^2Q^2}\right)\left(\frac{\rm NEP}{P_d}\right)^2, \tag{S-57}$$

$$\tag{S-58}$$

where η ($=0.67$ for our set-up) is the overall detection efficiency of the transmitted optical power, and again an optimal detuning point of $\Delta_o=\Gamma/2\sqrt{3}$ is assumed in transducing the mechanical motion. Minimizing the sum of $S_x^{\rm SN}$ and $S_x^{\rm BA}$ with respect to dropped optical power (assuming the two noise sources are independent, which they are strictly not in our measurement scheme), one finds (to within a factor of $4/3$) the *resonant* SQL for the displacement noise power spectral density, $S_{SQL}(\Omega_M/2\pi)=2\hbar Q_M/m_x\Omega_M^2$. A plot of the calculated different components of displacement sensitivity noise, on-resonance with the h_{1d} mechanical mode, are given in Fig. S-1 versus dropped optical cavity power for our system. The three differenent dropped cavity power levels used in the measurements presented in the main text are shown as black, vertical dashed lines (corresponding to 3.8, 38, and 1500 μW). The cyan horizontal dashed line is the resonant SQL. One can clearly see from this plot that the thermal noise swamps all other noise sources for the range of our measurements. In particular, at the power level used in the measurements displayed in Fig. 3 of the main text ($P_i=12.7$ μW, $P_d=3.8$ μW), the displacement noise sensitivity for our photoreceiver (5×10^{-17} m/Hz$^{1/2}$) is within a factor of four of the SQL (quantum-back action noise is below the SQL at this power level).

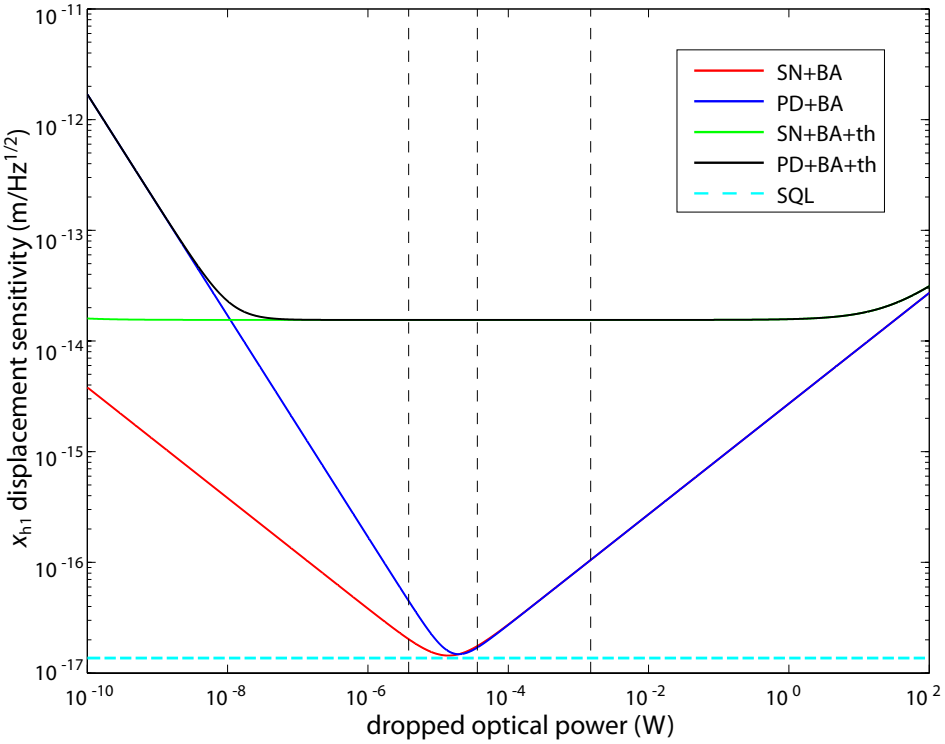

FIG. S-1: **Theoretical plot of the on-resonance displacement noise components for the h_{1d} mechanical mode**. The various component labels are: SN=shot noise, PD=photoreceiver noise, th=thermal noise, BA=quantum back-action. The parameters for the detection scheme are $\eta = 0.67$, NEP= 2.5 pW/Hz$^{1/2}$, $\Delta_o = \Gamma/2\sqrt{3}$, and $K = 0.09$. The parameters used for the h_{1d} mode are $\Omega_M/2\pi = 7.9$ MHz, $Q_M = 80$, and $g_{\rm OM}/2\pi = 123$ GHz/nm. The zipper optical cavity properties are $Q = 28,000$, $Q_i = 30,000$, and $\lambda_o = 1543$ nm.

III. THERMO-MECHANICAL EFFECTS

It is also important to consider thermo-mechanical effects (i.e., direct mechanical actuation stemming from thermal effects such as the pressure rise in the gas between the zipper nanobeams or thermal expansion of the nanobeams and surrounding supports)[4]. Thermo-mechanical effects can not only produce a temperature dependent shift in the cavity resonance frequency as described above in the case of the thermo-optic effect, but in addition they can directly produce a force on the nanobeams. On first blush, one might expect that thermo-mechanical effects are responsible for the blue-detuned damping measured in the zipper cavities (for instance, the sign of a thermo-mechanical force due to the pressure rise in the gas between the nanobeams would be opposite that of the optical force). However, even an overly optimistic estimate of the magnitude of thermo-mechanical effects indicates that this is not the case.

The steady-state temperature rise inside the cavity at the largest optical input powers used in this work ($P_i = 5$ mW) is roughly $\Delta T_0 = 60$ K (estimated from the measured thermal tuning rate of the cavity as described below). The optical energy inside the cavity is being modulated by roughly $\beta = 15\%$ of the time-averaged internal cavity energy due to thermal motion of the nanobeams. The component of the zipper cavity temperature oscillating in-phase with the optical cavity energy at the mechanical frequency ($\Omega_M \sim 10$ MHz) is roughly $\Delta T_q \sim (\gamma_{th}/\Omega_M)^2\beta\Delta T_0$, whereas the in-quadrature component of the zipper cavity temperature is $\Delta T_p \sim (\gamma_{th}/\Omega_M)\beta\Delta T_0$. This assumes of course that $\gamma_{th} \ll \Omega_M$, as is the case for the zipper cavity. Using some of the numbers estimated below, we find $\gamma_{th}/\Omega_M \sim 10^{-3}$, so that the in-phase and in-quadrature modulations in the cavity temperature are at most $\Delta T_q \sim 10^{-5}$ K and $\Delta T_p \sim 10^{-2}$ K, respectively.

We first consider a thermo-mechanical force from the thermal expansion in the nanobeams. The resulting in-plane displacement (which couples to the optical field) is difficult to simply estimate as it sensitivitly depends upon the beam clamping. We have performed finite-element-method (FEM) simulations of our stuctures, with an accurate representation of our clamping geometry, and find that the resulting in-plane displacement is $\delta x = 80$ pm for $\Delta T_0 = 60$ K at the center of the zipper cavity. From the above estimated in-phase and in-quadrature temperature oscillations for this static temperature shift, we find the corresponding in-phase and in-quadrature thermo-mechanical displacements, $\delta x_q \sim 1.3 \times 10^{-17}$ m and $\delta x_p \sim 1.3 \times 10^{-14}$ m, respectively. The effective in-plane force producing these in-plane displacements is related to the spring constant of the structure, and given by, $\Delta F \sim m_x \Omega_M^2 \delta x$. Putting this all together, we arrive at in-phase and in-quadrature (relative to the mechanical oscillation)

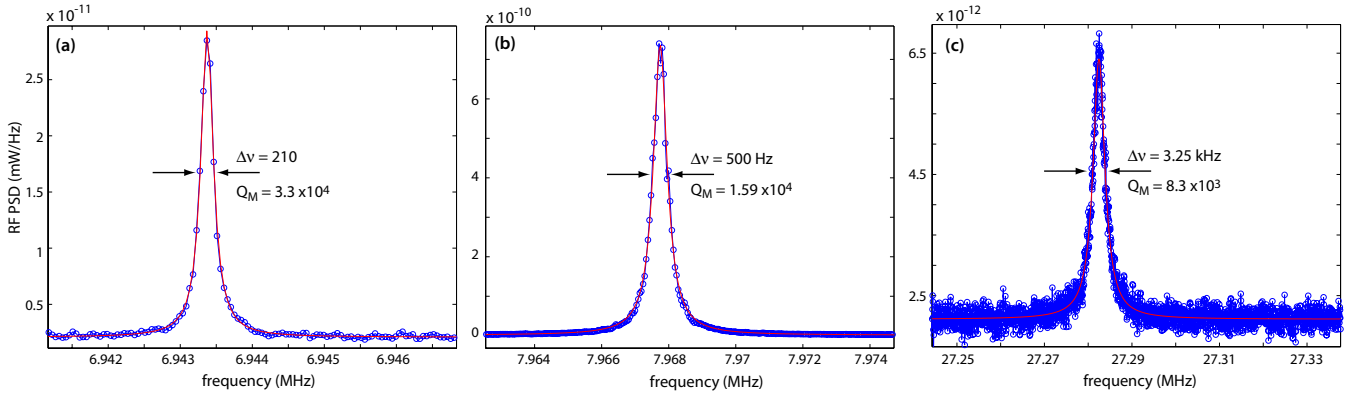

FIG. S-2: **Vacuum measurements of mechanical Q-factor of zipper cavity PCCC30a$_{\mathbf{fov}_{2,3}-\mathbf{dev}_{19,5}}$ (device in main text)**. **a**, fundamental vertical displacement mode, ν_1, **b**, fundamental in-plane displacement mode, h_1, and **c**, third-order in-plane displacement mode, h_3. Measurements were performed in a vacuum of $\sim 10^{-6}$ Torr, and at an optical input power of $P_i \sim 1$ μW, well below the optical power level where optomechanical amplification/damping is significant. This was confirmed by performing both blue and red detuned measurements.

components of in-plane force on the nanobeams equal to $\Delta F_q \sim 1.3\times10^{-15}$ N and $\Delta F_p \sim 1.3\times10^{-12}$ N. The corresponding corrections to the mechancical frequency and damping of the mechanical motion are given by, $\Delta(\Omega_M^2) \sim \Delta F_q/(m_x\sqrt{2}x_{rms})$ and $\Delta(\gamma_M) \sim \Delta F_p/(m_x\Omega_M\sqrt{2}x_{rms})$, where $x_{rms}\approx 6$ pm is the thermal rms amplitude of motion in our case. For $\Omega_M/2\pi = 8$ MHz and $\gamma_M/2\pi = 150$ kHz of the unperturbed zipper cavity h_{1d} mode, we find $\Delta(\Omega_M^2)/\Omega_M^2 \sim 1.4\times10^{-6}$ and $\Delta(\gamma_M)/\gamma_M \sim 7.5\times10^{-2}$. The measured (frequency)^2 shift is $\sim 10^6$ times larger than this estimate, indicating that the measured spring effect is not a result of this sort of thermo-mechanical coupling. The measured mechanical damping factor is $\Delta\gamma_M/\gamma_M \sim 8$, which is two-orders of magnitude larger than can be expected from thermo-mechanical coupling due to thermal expansion of the nanobeams.

Another possible thermo-mechanical force is that due to the temperature dependent pressure changes in the gas (nitrogen) surrounding the nanobeams. Treating a worst case scenario in which the gas between the nanobeams is unable to expand (molecules cannot escape), the in-phase and in-quadrature pressure increases would be approximately $\Delta P_q \sim (\Delta T_q/T_0)P_0 \sim 3\times10^{-8}P_0$ and $\Delta P_p \sim (\Delta T_p/T_0)P_0 \sim 3\times10^{-5}P_0$, respectively, near room temperature ($T_0 = 300$ K). The area of the gap-side of the nanobeams in the zipper cavity is 10^{-11} m^2, yielding a best-case scenario in-phase and in-quadrature force of $\Delta F_q \sim 3\times10^{-14}$ N and $\Delta F_p \sim 3\times10^{-11}$ N, respectively. The corresponding corrections to the mechancical frequency and damping of the mechanical motion are $\Delta(\Omega_M^2)/\Omega_M^2 \sim 3\times10^{-5}$ and $\Delta(\gamma_M)/\gamma_M \sim 1.7$. Again, the measured (frequency)^2 shift is $\sim 10^5$ times too small to account for the measured spring effect. The predicted mechanical-amplitude damping factor is within an order of magnitude of the measured value, although still a factor of 5 times too small even with the extremely "optimistic" estimate for the pressure rise. As such, it is unlikely that this thermo-mechanical effect is contributing significantly to the observed mechanical damping either.

A final comment relates to the difference between the thermo-optic effect studied here and direct thermo-mechanical damping/amplification present in other nanomechanical and cavity-optomechanical devices[4,5]. In these previously studied devices, if the pure optical force were removed the system would behave in a similar fashion. In the case of the thermo-optic effect, the thermo-optic tuning only serves to enhance or quench the bare optomechanical coupling, effectively riding on top of the optomechanical response. Turning off the optical force, then, eliminates the coupling of the thermo-optic effect to the mechanical degrees of freedom of the system.

IV. VACUUM MEASUREMENTS OF THE ZIPPER CAVITY MECHANICAL PROPERTIES

Gas damping in the zipper cavity structure can be expected to be significant due to the proximity of the nanobeams forming the cavity and the squeeze-film damping of trapped gas in the gap between the beams[6]. Measurements presented in the main text were all performed in a nitrogen-purged acrylic box, and the mechanical Q-factor of all of the mechanical modes were measured to be within a range of $Q_M = 50$-150. In the main text we hypothesize that the Q-factors are limited by gas damping. This was based upon an estimate of the gas damping at atmosphere, and the fact that we noticed interesting effects that could likely be attributed to gas damping, such as mechanical linewidth differences between common and differential modes.

In order to more clearly separate gas damping from other more intrinsic damping mechanisms (such as clamping and thermoelastic losses) we have performed measurements of the optically-transduced RF spectrum of the zipper cavity in a vacuum of

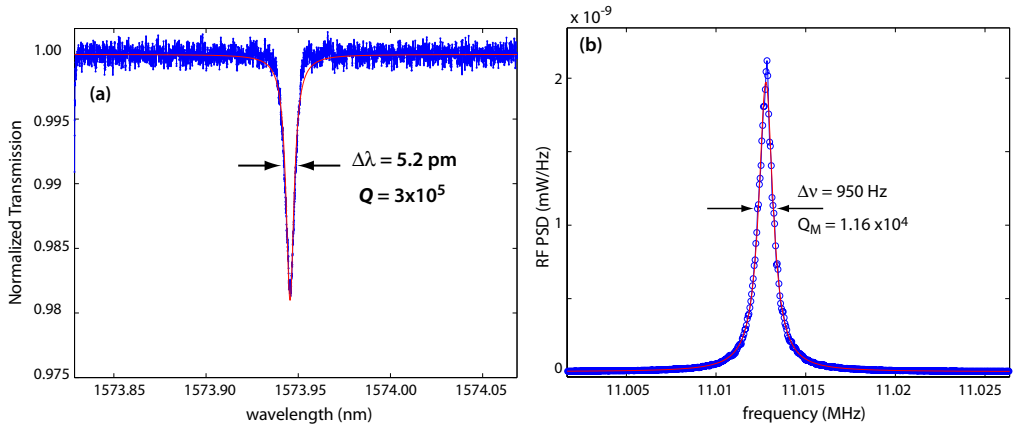

FIG. S-3: **Vacuum measurements of zipper cavity PCCC38c$_{\mathbf{fov_{1,5}-dev_{5,4}}}$.** **a**, Optical wavelength scan of the TE$_{+,1}$ mode, indicating an optical Q-factor of 3×10^5. **b**, Optically-transduced RF spectrum of the fundamental in-plane displacement mode, h_1. Measurements were again performed in a vacuum of $\sim10^{-6}$ Torr, and at an optical input power of $P_i\sim1$ μW, well below the optical power level where optomechanical amplification/damping is significant. This was confirmed by performing both blue and red detuned measurements.

roughly 10^{-6} Torr (well above that where gas damping plays a role). We performed measurements on both the device studied in detail in the main text (PCCC30a$_{\mathrm{fov_{2,3}-dev_{19,5}}}$), and another device from a later generation of samples (PCCC38c$_{\mathrm{fov_{1,5}-dev_{5,4}}}$). This second device was chosen because of the clear difference in the quality of the plasma dry etched holes in the nanobeams. Later generation samples used a more optimized plasma dry etch resulting in significantly less mask erosion and damage to the sidewall and inner holes of the patterned nanobeams. Figure S-2 shows the measured linewidth of several different mechanical modes for device PCCC30a$_{\mathrm{fov_{2,3}-dev_{19,5}}}$ and Fig. S-3 shows both the optical and mechanical spectrum for the later generation device, PCCC38c$_{\mathrm{fov_{1,5}-dev_{5,4}}}$.

The estimated in-vacuum mechanical Q factor from the fit linewidth for the v_1, h_1, and h_3 modes of device PCCC30a$_{\mathrm{fov_{2,3}-dev_{19,5}}}$ are $Q_M=3.3\times10^4$, 1.6×10^4, and 8.3×10^3, respectively. These room temperature mechanical Q factors are within a factor of 3-6 of the highest reported values for similar geometry (length) nanobeams formed from stoichiometric, high stress, LPCVD silicon nitride[7], and are higher than previously measured values for nanobeams in non-stressed nitride films. For device PCCC38c$_{\mathrm{fov_{1,5}-dev_{5,4}}}$ we see that the optical Q-factor has been significantly improved over earlier devices to $Q=3\times10^5$ (corresponding to a Finesse of $\mathcal{F}\sim10^5$), whereas the mechanical Q-factor of the h_1 in-plane mechanical mode is slightly lower at $Q_M=1.16\times10^4$. Although difficult to estimate, the lower mechanical Q-factor is likely due to the wider nanobeams of device PCCC38c$_{\mathrm{fov_{1,5}-dev_{5,4}}}$ (and hence slightly different clamping loss), and there is not likely a strong correlation between the etching of holes in the nanobeams and the resulting mechanical Q-factor, at least at the level of mechanical dissipation measured here.

V. STEADY-STATE NONLINEAR OPTICAL MODEL OF THE *ZIPPER* OPTOMECHANICAL CAVITY

A. Optical properties

The fiber Mach-Zender interferometer is used to calibrate the wavelength scans of the zipper cavity modes. For the zipper cavity mode (TE$_{+,1}$) of the device studied in Fig. 2(c), Fig. 3, and Fig. 4 of the main text, the taper-loaded optical Q-factor was measured to be $Q_T=2.8\times10^4$ with a transmission contrast (fractional dropped power) of $\Delta T=27.5\%$. The resonance wavelength is $\lambda\sim1543$ nm. The fit value (see below) of the component of optical loss attributed to absorption is $Q_a=4.8\times10^5$.

B. Geometry

As discussed in the main text, the zipper cavity device under study had $l=36$ μm, $w=650$ nm, $s=120$ nm, and $t=400$ nm, as measured by calibrated SEM inspection. The etched air holes were measured to be 330 nm by 330 nm in area. The total number of air holes per beam is 55.

C. Silicon nitride material properties

The material properties of silicon nitride were scoured from a number of sources and journal articles. Where possible we have used parameters most closely associate with LPCVD silicon nitride on $\langle 100 \rangle$ Si. The density of LPCVD silicon nitride is taken to be $\rho = 3100$ kg/m^3, the Young's modulus $Y = 290$ GPa, the tensile stress $S = 1$ GPa, the coefficient of thermal expansion $\eta_{TE} = 3.3 \times 10^{-6}$ K^{-1}, the thermal conducivity $\kappa_{th} = 30$ W/m/K, and the specific heat $c_{sh} = 0.7$ J/g/K.

D. Thermal properties of the zipper cavity

Due to the air-filling-fraction of the etched holes in the zipper cavity nanobeams, the thermal conductivity of the patterned beams was taken as $\Gamma_{th} = 50\%$ of the bulk value. A simple estimate for the thermal resistance of the zipper cavity is then given by $R_{th} \sim l/(8tw\Gamma_{th}\kappa_{th}) \approx 1.15 \times 10^6$ K/W, where the factor of $1/8$ comes from the ability for heat to escape out either end of the nanobeams and in either direction (note that FEM simulations of the effects of convection and conduction by the surrounding nitrgen gas indicate that the thermal resistance of the zipper cavity is dominated by conduction in the nitride film). The physical mass of the zipper cavity, taking into account the etched holes, is approximately $m = 43$ picograms. The heat capacity of the zipper cavity is then roughly $c_h = 3 \times 10^{-11}$ J/K. From the heat capacity and the thermal resistance, the thermal decay rate is estimated to be $\gamma_{th} = 1/R_{th}c_h \sim 2.9 \times 10^4$ s^{-1}. Finite-element-method simulations of thermal properties of the zipper cavity yield an effective thermal resistance of $R_{th} = 1.09 \times 10^6$ K/W and a thermal decay rate of $\gamma_{th} = 1/R_{th}c_h = 5.26 \times 10^4$ s^{-1} for temperature at the center of the zipper cavity, in reasonable correspondence to the estimated values. The thermal tuning rate (dominated by the thermo-optic effect) for the device under study was measured to be $\delta\lambda_c/\delta T = 0.0149$ nm/K using a thermo-electrically heated stage and a thermo-couple placed a few millimeters from the sample.

E. Optomechanical properties of the zipper cavity

The bare mechanical resonance frequency of the h_{1d} zipper cavity is measured to be $\Omega_M \sim 8$ MHz, in good corresondence with the FEM-simulated value when $S = 1$ GPa of tensile stress is introduced into the silicon nitride film. The measured mechanical Q-factor, in the nitrogen-purged test set-up, is approximately $Q_M \approx 50$ for the differential mode, and roughly $Q_M \approx 150$ for the common mode of motion of the nanobeams. This difference is attributed to the squeeze-film-like damping[6] of the differential motion due to gas "squeezed" in between the beams. The FEM-simulated optomechanical coupling length, based upon SEM images of the device under test, is $L_{\rm OM} = 2.09$ μm. The inferred optomechanical coupling length value, based upon the peak measured optical spring effect for various optical input powers, is $L_{\rm OM} = 1.575$ μm. Although good correspondence is found between simulated and measured $L_{\rm OM}$, the measured value of $L_{\rm OM} = 1.575$ μm is used to fit the remaining cavity parameters as described below.

F. Wavelength scan fitting

The steady-state equations of motion of the zipper cavity, as given by eqs. (S-9-S-11), are numerically solved with variable absorption-limited cavity Q-factor, Q_a (all other parameters are fixed to values given above). The resulting wavelength dependent transmission curve is then fit to the measured (low-pass filtered) curve for a variety of optical input powers in order to determine the fit value of Q_a ($= 4.8 \times 10^5$). Optical input power is calibrated as described in the Methods section using a calibrated power meter and measuring the system response for optical power sent in both directions down the fiber taper. From the fit transmission curve (Fig. 4(a)), the laser-cavity detuning (Fig. 4(b)) at each point within the intensity image of Fig. 4(c) can be determined. Calculating the optomechanical damping versus laser-cavity detuning, with and without the thermo-optic correction, is then used to model the expected RF power in the mechanical resonance line using eqs. (S-43-S-46).

---

* Electronic address: opainter@caltech.edu; URL: http://copilot.caltech.edu

1 T. J. Kippenberg and K. Vahala, Optics Express **15**, 17172 (2007).

2 I. Tittonen, G. Breitenbach, T. Kalkbrenner, T. Müller, R. Conradt, S. Schiller, E. Steinsland, N. Blanc, and N. F. de Rooij, Phys. Rev. A **59**, 1038 (1999).

3 P. E. Barclay, K. Srinivasan, and O. Painter, Opt. Express **13**, 801 (2005).

4 B. Ilic, S. Krylov, K. Aubin, R. Reichenbach, and H. G. Craighead, Appl. Phys. Lett. **86** (2005).

5 C. Höhberger and K. Karrai, Nature **432**, 1002 (2004).

6 J. B. Starr, Techn. Digest IEEE Solid State Sensor and Acuator Workshop (Hilton Head Island, SC, 1990) pp. 44–47 (1990).

7 S. S. Verbridge, J. M. Parpia, R. B. Reichenbach, L. M. Bellan, and H. G. Craighead, J. Appl. Phys. **99** (2006).